Original Paper

phys. stat. sol. (a) **203**, No. 4, 659–669 (2006) / **DOI** 10.1002/pssa.200564508

Wafering of silicon crystals

H. J. Möller*

Institute for Experimental Physics, Technische Universität Bergakademie Freiberg, Leipziger Str. 23, 09599 Freiberg, Germany

Received 19 September 2005, accepted 15 December 2005
Published online 14 March 2006

PACS 62.20.Mk, 62.20.Qp, 81.65.–b

Multi-wire sawing is the main slicing technique for large multi- and monocrystalline silicon crystals in the photovoltaic and microelectronic industry. This paper describes the basic mechanisms by which slicing is achieved and develops a model for the material removal rate. It is shown that the hydrodynamic behavior of the slurry and the elastic interaction with the wire are an important aspect that has to be taken into account. The material removal occurs by the indentation of free floating SiC particles under the pressure of the wire. The microscopic fracture processes under the indented particles have been investigated and are described quantitatively. The numerical and experimental results are compared.

1 Introduction

Multi-wire sawing is the main slicing technique for large multi- and monocrystalline silicon crystals in the photovoltaic and microelectronic industry [1]. The advantages over other techniques are a high throughput, a small kerf loss, less restrictions on the size of the ingots, and a good surface quality. Currently solar cell wafers are cut with a thickness between 250 and 350 μm, but a thickness down to about 100 μm can be achieved by the technique. While in the last years the cost of solar cell processing and module fabrication could be reduced considerably, the sawing costs remain high, about 30% of the wafer production [2]. The incentive to optimize the sawing technique for further cost reduction in mass production is thus high. The sawing process depends on several variable parameters, which makes it difficult to optimize the process in view of throughput, material losses, reduction of supply materials and wafer quality. Basic knowledge about the microscopic details of the sawing process is required in order to slice crystals in a controlled way. In the following the principles of the sawing process will be described as far as they are understood at present. It will be shown that the hydrodynamic behavior of the slurry between wire and crystal surface is an important aspect that has to be taken into account.

2 Multi-wire wafering technique

The principle of the multi-wire technology is depicted in Fig. 1. A single wire is fed from a supply spool through a pulley and tension control unit to the wire guides that are grooved with a constant pitch. Multiple strands of a wire net are formed by winding the wire on the wire guides through the 500–700 parallel grooves. A take-up spool collects the used wire. The wire is pulled by the torque exerted by the main drive and slave. The tension on the wire is maintained by a feedback control unit. The silicon crystal on the holder is pushed against the moving wire web and sliced into hundreds of wafers at the same time.

* e-mail: moeller@physik.tu-freiberg.de

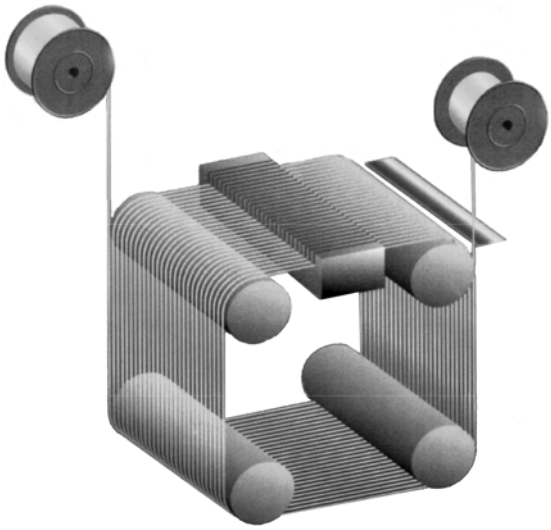

Fig. 1 Schematic diagram depicting the principle of the multi-wire sawing technique. The crystal is pushed against the wire web with a constant feeding rate, which is equal to the sawing rate in the steady state. The resulting wire bow determines the force on the wire and the crystal.

Wafers are either cut by wires that are moving in one direction or by oscillating wires. Cutting in one direction allows higher wire speeds between 5 to 15 m/s but yields less planar surfaces.

Cutting is achieved by an abrasive slurry which is supplied through nozzles over the wire web and carried by the wire into the sawing channel. The slurry consists of a suspension of hard lapping particles. Today SiC powders are the most commonly used abrasives. The material is very expensive and accounts for 25–35% of the total slicing cost. The volume fraction of solid SiC particles can vary between 30–50% and the mean grain size between 5–30 μm. The main purpose of the slurry is to transport the abrasive particles into the sawing channels and to the crystal surface. Most of the commercial slurries are based on oil or ethylene glycol. The entry of the slurry is a result of the interaction between the wire and the highly viscous slurry. Normally only a small amount of slurry enters the cutting zone. The factors that are important here are the viscosity and the wire speed, but to understand the fluid mechanical problems that are involved a complex physical modeling is required. First attempts of a description have been reported recently [3–8].

Material is continuously removed through the interaction of the SiC particles below the moving wire and the silicon surface. The abrasive action of the SiC depends on many factors such as wire speed, force between wire and crystal, the solid fraction of SiC in the suspension, the viscosity of the suspension, the size distribution and the shape of SiC particles. The viscosity of the slurry depends on the temperature and the solid fraction of particles, which changes because of the continuous abrasion of silicon and iron from the wire.

The kerf loss and surface quality are determined by the diameter of the wire, the size distribution of the SiC particles and possible transverse vibrations of the wire [9]. Typical diameters of steel wires are around 170 μm. This yields kerf losses around 200–250 μm per wafer.

The objective of efficient sawing is to slice with a high throughput, with a minimum loss of slurry and silicon, and with a high quality of the resulting wafers. Since many parameters can be changed the optimization of sawing is a difficult task and today mainly done by the wafer manufacturers. They are mostly guided by experience. In the following the main results of investigations are summarized which describe the current understanding of the microscopic details of the wire sawing and yield some guidelines to optimize the process.

3 Basic sawing mechanism

The main results of the experimental investigations are summarized here and describe the current understanding of the microscopic details of the wire sawing process. Figure 2 shows schematically the situa-

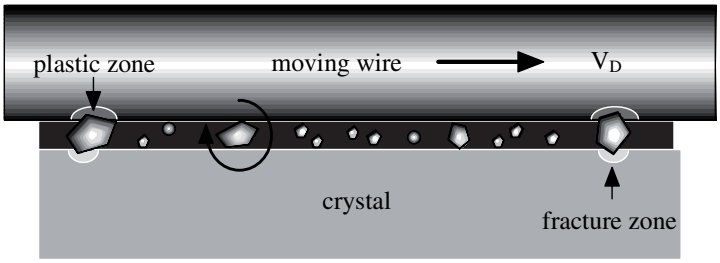

Fig. 2 Schematic diagram of wire, slurry with abrasive, and crystal in the cutting zone. Under external force the wire bows and exerts forces on the particles and the slurry.

tion in the sawing channel. The space between wire and crystal surface is filled with slurry and abrasive particles. The crystal is pushed against the wire web and causes a bow of the wire. The bow angle varies typically between 1–5 deg. The resulting pressure of the wire varies along the contact area. The forces are maximum directly below the wire and decrease towards the side faces. Because of the observed transverse vibrations of the wire additional forces may be exerted sideward. The cutting process at the side faces is important because it determines the final surface quality of the sliced wafers.

The microscopic material removal process can be explained by the interaction of loose, rolling SiC particles that are randomly indented into the crystal surface until small silicon pieces are chipped away. Since SiC particles are facetted and contain sharp edges and tips, they can exert very high local pressures on the surface. This "rolling – indenting grain" model forms the physical basis of the wire sawing process. Similar surface structures also occur after lapping surfaces of brittle materials with loose abrasive particles [10, 11]. A review of material removal mechanisms can be found in Refs. [12, 13].

The individual process of the interaction of a single particle with sharp edges and the surface of a brittle material has been studied by micro-indentation experiments [14]. The main results are summarized schematically in Fig. 3 for a "sharp" indenter with a pyramid geometry. Loading by sharp indenters first leads to the generation of a remnant plastic impression in the surface known as the elastic–plastic zone. The extension of the plastic zone depends on the hardness of the material. With increasing pressure the material begins to break and so-called median and radial cracks are generated parallel to the load axis along certain crystallographic planes emanating from the plastic zone. These cracks may coalesce and form half-penny cracks that extend to the surface. The extension of the cracks is determined by the fracture toughness of the material. Upon unloading residual stresses between the highly deformed plastic zone and the bulk lateral cracks parallel to the surface can be initiated below the plastic zone. When these lateral cracks reach the surface material is chipped away. This is the main process for material removal during sawing. The volume that is removed depends on the applied force by a power law as has been determined experimentally in Ref. [6].

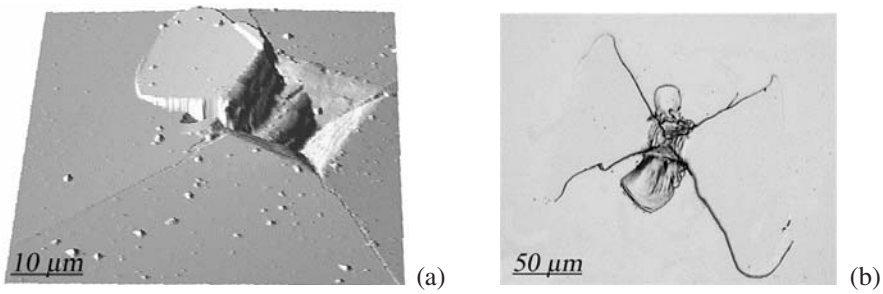

Fig. 3 (a) Atomic force microscope image of the plastic zone under a Vickers indenter. (b) Crack system, which develops under the indenter at higher loads: median/radial cracks, which extend perpendicular to the surface, and lateral cracks parallel to the surface, which remove material.

When material is removed by chipping the median and radial cracks still remain, because they reach much deeper than the extension of the plastic zone, which determines approximately the depth of the material removal. This crack system is part of the saw damage which has to be removed for further processing of the wafers. Combining the rolling-indenting process of free abrasive grains with the fracture mechanics of brittle materials a quantitative descriptions of the material removal process could be derived, which will be described next.

3.1 Elasto-hydrodynamic behavior of slurry and wire

The global behavior of the abrasive particles is controlled by the hydrodynamic conditions in the slurry film between ingot surface and wire. The slurry transports the abrasive particles into the cutting zone and determines the force acting upon the grains. Depending on the film thickness between wire and surface, the particles are either in direct contact with both the wire and the surface (semi-contact case) or the particles are floating freely (non-contact case). In the first case the force on the grains is exerted by the wire directly whereas in the second case the force is supplied by the shear stress or other factors in the moving slurry. It is also evident that if the slurry film thickness is much lower compared to the average size of the abrasive grains less particles would enter the cutting zone, thus leading to very low sawing rates and the risk of wire rupture due to dry friction.

It is therefore necessary to determine the slurry film thickness under the various sawing conditions. The hydrodynamic behavior of slurry films has been studied in lubrication or polishing processes, where many fundamental aspects have been derived from experimental and theoretical results [15, 16]. An important aspect is that the work tool and the crystal can deform elastically in response to the slurry pressure. Considering that the wires are thin and long it is very likely that the elastic response of the wire has to be considered when the slurry transport is analyzed. In the following some main aspect shall be derived from a one dimensional treatment of the hydrodynamic slurry transport.

The space between wire and crystal surface is filled with slurry, which is transported by the moving wire. The starting point to describe the slurry flow under steady conditions is the Reynolds equation. In the one-dimensional case we have

$$\frac{\partial}{\partial x}\left(\frac{h^3}{\eta}\frac{\partial p}{\partial x}\right) = 6\,v\,\frac{\partial h}{\partial x}, \tag{1}$$

where x is the coordinate along the wire (Fig. 4), $h(x)$ the distance between wire and crystal surface, v the wire velocity, η the slurry viscosity, and $p(x)$ the hydrodynamic slurry pressure. Integration of the equation yields

$$\frac{\partial p}{\partial x} = 6v\eta\,\frac{h - h_0}{h^3}, \tag{2}$$

h_0 is the integration constant and derived from the condition that the derivative of p is zero for $h = h_0$. The hydrodynamic pressure in the slurry exerts forces on the wire, which may bend and deform elastically then. Like a pulled string the bow of the wire yields a backward force, which is determined by the local curvature $y''(x)$, where $y(x)$ is the vertical displacement (Fig. 4). The derivative of the force component T_n normal to the wire determines the local curvature by the following equation:

$$y'' = -\frac{1}{T}\frac{\partial T_n}{\partial x}, \tag{3}$$

where T is the tensile force along the wire. If the normal component is constant everywhere $(T_n = T_n^0)$ the wire assumes a circular shape with a uniform curvature radius r_0:

$$T_n^0 = \frac{2a}{r_0}T, \tag{4}$$

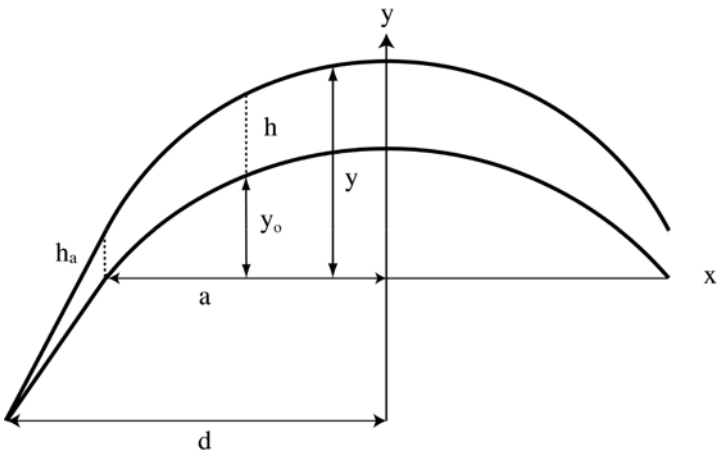

Fig. 4 Schematic diagram of the wire bow $y(x)$ and the crystal surface $y_0(x)$ along the cutting zone from $x = -a$ to a. The wire is fixed at the ends at $x = -d$ to d. It is assumed here that the crystal surface has a circular shape, whereas the wire shape is determined by the elastic interaction between wire and the pressure in the slurry film.

$a = l_0/2$ where l_0 is the cutting length. If slurry fills the space between wire and crystal and a hydrodynamic pressure builds up due to the flow conditions, the wire will be pushed up by a certain distance h and assume such a shape that the local forces exerted by the hydrodynamic pressure, which varies along the wire, and the normal force components T_n of the bent wire are balanced locally. In this case T_n is no longer constant but varies along the wire.

SiC particles in the slurry, which are in direct contact with the wire and the crystal surface are pushed into the surface by the local force $F_N = T_n$. Since the material removal process depends on the forces F_N, the removal rate will vary along the crystal surface correspondingly. In a steady state situation however, cutting of the wire through the crystal occurs at a constant rate along the wire. This is only possible if the crystal surface adopts a shape such that the normal force is constant everywhere and material removal occurs at the same rate.

Investigations of the shape of the surface during cutting have shown that it is slightly bent and deviates only very little from a circular shape. Therefore we assume in the following that the crystal surface has a constant curvature with radius r_0, which can be described by a circular segment $y_0(x)$. The distance h between crystal surface and wire, which is the width of the slurry transport channel, is determined then by (Fig. 4)

$$h(x) = y(x) - y_0(x) \,. \tag{5}$$

The pressure below the wire can be determined from Eq. (3). Assuming a constant pressure p^* below a wire of radius R it can be expressed by

$$p^* = \frac{1}{\pi R} \frac{\partial T_n}{\partial x} \,. \tag{6}$$

Considering however the cross section of the sawing channel, the pressure below the wire changes from a maximum value directly below the wire towards the side faces where the pressure must be zero at the free surfaces of the fluid bed. Thus the actual average pressure p will be lower because of the decreasing pressure towards the side faces. If we take $p = \alpha p^*$ (with $\alpha < 1$) one can derive with Eq. (3) and Eq. (5)

$$p = -\frac{T}{\pi \alpha R} \left(\frac{\partial^2 h}{\partial x^2} + \frac{\partial^2 y_0}{\partial x^2} \right), \tag{7}$$

α has to be determined from a three dimensional treatment of the hydrodynamic problem. Here it is taken as a free parameter. In equilibrium between wire and slurry the pressures in Eq. (2) and Eq. (7) have to be equal. Since the curvature of y_0 is constant the third derivative is zero and one obtains

$$\frac{\partial^3 h}{\partial x^3} + \frac{6\pi v \eta \alpha R}{T} \frac{h - h_0}{h^3} = 0 . \tag{8}$$

In order to solve the differential equation one needs appropriate boundary conditions. From Eq. (7) together with (3) and (4) one derives with the cutting length $l_0 = 2a$

$$\frac{\partial^2 h}{\partial x^2} = -\frac{\pi \alpha R}{T}(p - p_0) \quad \text{and} \quad p_0 = \frac{T_n^0}{\pi \alpha l_0 R} . \tag{9}$$

We assume that the pressure in the slurry at the exit of the sawing channel is zero: $p(a) = 0$. This yields

$$\frac{\partial^2 h}{\partial x^2}(a) = \frac{\pi \alpha R}{T} p_0 . \tag{10}$$

The pressure $p(-a) = p_a$ at the entry is determined by the build-up of slurry, which is carried by the wire to the cutting zone. The entry pressure p_a has been estimated approximately by [4]

$$p_a \approx \frac{\rho v^2}{3} , \tag{11}$$

where ρ is the density of the slurry and v the wire velocity. The second boundary condition can be written then

$$\frac{\partial^2 h}{\partial x^2}(-a) = -\frac{\pi \alpha R}{T}(p_a - p_0) . \tag{12}$$

A third condition can be derived from the integration of Eq. (9) between $x = -a$ to a which yields

$$h'(a) - h'(-a) = -\frac{\pi \alpha l_0 R}{T}(\bar{p} - p_0) , \tag{13}$$

where $\bar{p}$ is the average total pressure in the slurry, which is a function of h_0. Since h_0 will be determined from the final solution, an iterative procedure is necessary to find the correct value.

A starting value can be obtained from geometrical considerations. The results show that for typical values of the input parameters the distance h differs only little from h_0, therefore one can approximately determine h_0 from the wire distance at the entry and exit region (Fig. 4). Since the position of the wire is fixed at the spools, located at a distance $x = \pm d$ from the center of the wire, the distance h can be related to the slopes of the wire at $x = \pm a$ by

$$\frac{h(\pm a)}{d - a} = y'(\pm a) - y_0'(\pm a) = \mp h'(\pm a) . \tag{14}$$

With $h_0 \approx (h(a) + h(-a))/2$ one obtains

$$h_0 \approx \frac{\pi \alpha l_0 R (d - a)}{T}(\bar{p} - p_0) . \tag{15}$$

This shows that the pressure difference $\bar{p} - p_0$ keeps the wire above the surface at the average distance h_0.

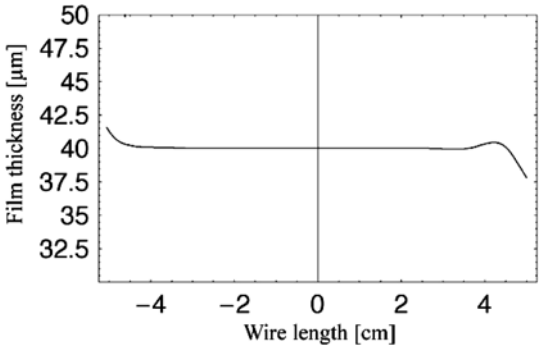

Fig. 5 Numerical calculation of the slurry film thickness $h(x)$ along the wire. The slurry entry is at $x = -5$ here. The parameters are given in the text.

3.2 Numerical results

The differential Eq. (8) together with the boundary conditions (10), (12) and (13) has been solved numerically with the following parameters: cutting length $l_0 = 10$ cm, spool distance $2d = 30$ cm, effective wire radius $\alpha R = 10$ µm, wire speed $v = 10$ m/s, viscosity $\eta = 100$ cP, wire tension $T = 50$ N, vertical wire force $F_{\text{tot}} = T_n^0 = 1$ N and an entry pressure $p_a = 0.0127$ MPa, which corresponds to a normal force of $T_n = 0.04$ N. These values correspond to parameters that are used in typical wire sawing experiments. A starting value for h_0 is chosen and then $h(x)$ determined from Eq. (8). The pressure $p(x)$ and the mean pressure $\overline{p}$ are calculated from Eq. (7). h_0 is varied then until Eq. (13) is fulfilled. The actual shape of the wire is calculated from $y(x) = y_0(x) + h(x)$.

Figure 5 shows the slurry film thickness along the wire position x. Apart from the entry and exit region the thickness remains almost constant. The comparison with the shape of the crystal surface, given by $y_0(x)$ indicates that the wire is almost parallel to the crystal surface. The mean film thickness is about 40 µm in this case. The slight deviations from this value are however responsible for the hydrodynamic pressure p which carries the wire. The pressure distribution is shown in Fig. 6.

The results show an almost constant pressure over most of the wire length. A maximum occurs in the exit region before the pressure drops to zero at the exit ($x = a$). The pressure in the entry region increases from $p = p_a$ to the mean value of about 0.31 MPa. One can see from the calculation, that only slight changes of the film thickness and the curvature of the wire are necessary to balance the pressure changes in the slurry.

An important result of the calculation is that the film thickness of about 40 µm is in the same range as the largest particles in conventional SiC particle distributions used for industrial wire sawing processes. Therefore one can assume that over the entire length of the wire the largest of the abrasive particles are in direct contact with wire and ingot. This result is important in view of the forces that are exerted on the particles and the modeling of the sawing process. In the following it is thus assumed that the largest particles in the size distribution are indented in the crystal surface and lead to material removal.

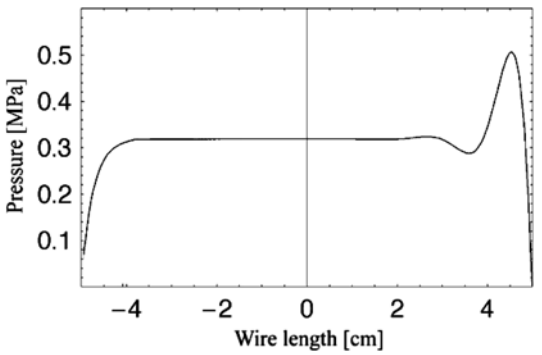

Fig. 6 Calculated hydrodynamic pressure $p(x)$ in the slurry film along the wire.

3.3 Material removal rate

The material volume V_0 that can be removed by lateral cracks at the impression of a single grain depends on the applied force F_N as has been shown in Ref. [6]:

$$V_0 \approx F_N^{(4n+1)/2} . \tag{16}$$

The exponent n has been determined experimentally for silicon and is $n = 0.85$, which gives $V_0 \approx F_N^{2.2}$. The sawing rate v_s, which is the thickness of a removed layer per unit time, can be calculated from the number of indentation events m per contact area A_s and time Δt multiplied by the volume of material V_0 that is removed in a single event

$$v_s = \frac{mV_0}{A_s \Delta t} . \tag{17}$$

If a rolling grain makes one indentation per cycle one can calculate the time interval for a single indentation from the angular velocity of the rotation. For a laminar flow of the slurry the mean angular velocity $f = 1/\Delta t$ can be determined from the linear velocity profile between crystal surface and moving wire and is given by $f = v/2\,L_0$ where L_0 is the average distance between wire and surface. Combining the equations yields for the sawing rate the fundamental relationship which forms the basis for the following theoretical descriptions

$$v_s = v_{s0}\, v\, m F_N^{(4n+1)/2} , \tag{18}$$

where the prefactor summarizes material and geometry parameters. The remaining problem that has to be solved is to determine the number m of indenting grains in the slurry and the normal force F_N acting upon each grain. Both factors can only be average values that have to be determined from the global stochastic behavior of many particles in the slurry under the external sawing conditions such as wire velocity v, wire load $F_{\text{tot}} = T_n^0$, particle size distribution or slurry concentration. These conditions shall be analyzed in the following.

3.4 Particle–surface interaction

In a slurry that contains free floating particles the load on the wire is exerted by the slurry and those particles that are in direct contact with wire and crystal surface. Depending on the film thickness either the slurry or the particles carries the main load. Only in the latter case the abrasive action can begin substantially. How many grains are in direct contact depends on the grain size distribution and the film thickness. Commercial SiC particle sizes can be described rather well by a Gaussian distribution (Fig. 7). It is evident because of the stiffness of the materials that wire and surface must be kept at a certain aver-

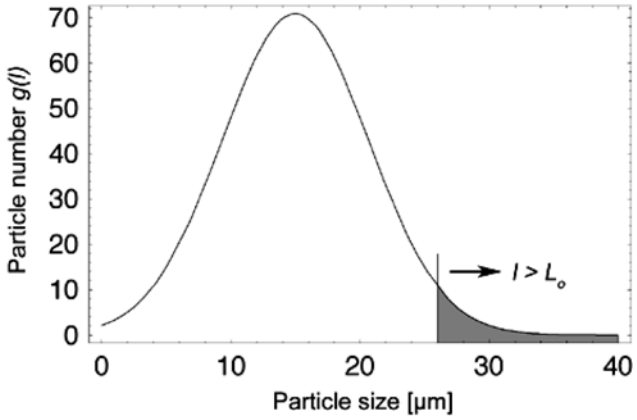

Fig. 7 Schematic particle size distribution $g(l)$. In the semi-contact case grains with a diameter $l > L_0$ are in contact both with wire and work piece surface. The total number of grains m in contact is proportional to the shaded area.

age distance L_0 which is mainly determined by the largest grains and the applied total force F_{tot}. The local changes in the distance $h(x)$, which have been calculated in Section 3.2, are neglected here. If the force F_{tot} is increased the average distance decreases and more grains come into contact with the surface. These grains are indented both into the wire and the crystal but in the following the indentation in the wire is neglected. The total force and number of particles m that are actually indented into the crystal surface can be derived from the particle size distribution $g(l)$ by the relation

$$F_{tot} = \int_{L_0}^{\infty} F(l - L_0)\, g\,(l)\, \mathrm{d}l\,. \tag{19}$$

F is the individual force on each particle in contact and m is equal to the integral over the shaded area in Fig. 7. The force F increases with the indentation depth $l - L_0$ for a particle with size $l > L_0$. The force law depends on the elastic and plastic behavior of particle and crystal surface. For Vickers indentations in brittle materials one obtains $F \approx (l - L_0)^2$ but other force law can be derived as well depending on the shape of the indented grains. Calculating Eq. (19) with a Gaussian size distribution for $g(l)$ one obtains the approximate equation

$$F_{tot} = mF_N\,, \tag{20}$$

where F_N is the average force on each particle in contact. The results of the calculations also show that F_N remains almost constant, which means that with increasing total force only the number m of indented particles increases. Inserting Eq. (20) in (18) yields the sawing rate v_s for the semi-contact case

$$v_s = v_{s0}^{sc}\, vF_{tot} F_N^{(4n-1)/2}\,. \tag{21}$$

With $n = 0.85$ one obtains for the sawing rate $v_s \approx vF_{tot} F_N^{1.2}$. The essential result from Eq. (21) is that in the semi-contact case the sawing rate is proportional to the wire velocity and wire load. The average particle force F_N, which depends on the shape and size distribution of the particles, remains constant. In the next chapter the main dependencies shall be compared with experimental results.

4 Experimental results

An industrial multi-wire saw equipped with force sensors has been used for the measurements. The oil slurry and SiC powders were commercial products. Figure 8 shows the sawing rate as a function of the applied wire load for different wire velocities. In both cases the sawing rate is proportional to the load. One can also observe that the material removal starts only above a certain threshold value of about 0.1 N. This can be explained with the minimum load for an abrasive particle that is required for the chipping mechanism to operate. Figure 9 shows the dependence on the wire velocity. In the typical velocity re-

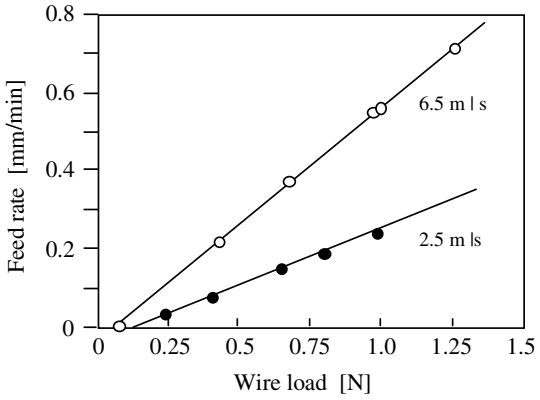

Fig. 8 Measurement of the sawing rate on an industrial multi-wire-saw as a function of the wire load for two different wire velocities. The material removal starts above a certain threshold value of about 0.1 N.

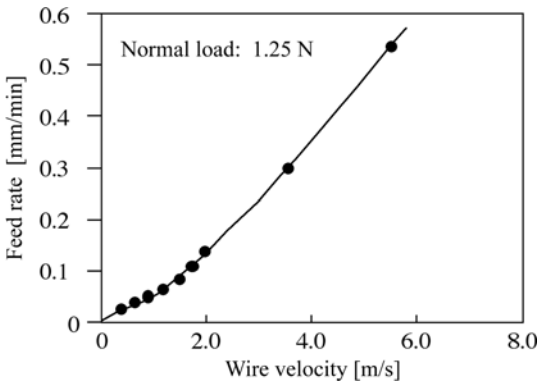

Fig. 9 Measurement of the sawing rate on an industrial multi-wire-saw as a function of the wire velocity for constant wire load.

gime of industrial multi-wire saws between 5–15 m/s a linear dependence is observed. For velocities below 2 m/s the dependence becomes non-linear and the slope decreases. Both results are in agreement with the predictions of Eq. (21) at least for higher speeds.

5 Summary

In the semi-contact case only the very large grains of a size distribution contribute to the sawing process. Estimations for typical commercial SiC powders show that these particles are about twice as large as the average size and their volume fraction is around 1% only. How many of the grains interact depends on the slurry film thickness and the hydrodynamic pressure. If the main load of the wire is carried by the film, either no particles are in contact or only little force is exerted on the particles. In both cases the resulting material removal rate will be rather low. If the film thickness decreases the larger particles begin to carry the main load and abrasive action begins. In this case the slurry is mainly responsible for the transport of the particles into the sawing channel. If the film thickness decreases further transport becomes more difficult and dry friction and wire rupture will occur.

The transition between the two load regimes depends on the flow properties of the slurry such as viscosity and impact pressure, and the other parameters such as wire speed, wire tension and the force, which presses the crystal against the wire. Under steady state conditions the material removal process can be described by the presented model. This is valid for a certain parameter range only. For instance if the film thickness decreases too much and particle transport is hindered other factors have to be considered. It is thus important to determine the limits of the model both theoretically and experimentally.

The hydrodynamic simulations have also shown that the distance between wire and crystal surface and the pressure vary particular in the entry and exit region. This indicates that the material removal process should differ in both regimes. In fact, it is known that the removal rate is higher in the entry region and the wafers are correspondingly thinner and rougher. This can be explained qualitatively by the reduced slurry pressure. In this case the particles have to carry more load which increases the removal rate.

The result of the hydrodynamic calculations show how the flow properties of the slurry contribute to the sawing process. One can expect that more realistic three dimensional calculations will reveal more details and help to improve the sawing process further.

Acknowledgements The experimental part of the work has been supported financially by the German BMBF and the Deutsche Solar AG under contract number 0329 667K/3.

References

[1] R. Wells, Solid State Technol. **30**, 63 (1987).
[2] A. Endrös, D. Franke, Ch. Häßler, J. Kaleis, W. Koch, and H. J. Möller, in: Handbook of Photovoltaic Engineering, edited by A. Luque and S. Hegedus (Wiley-VCH, Weinheim, 2002).

[3] R. K. Sahoo, V. Prasad, I. Kao, J. Talbott, and K. Gupta, ASME J. Electron. Packag. **120**, 131 (1998).
[4] M. Bhagavat, V. Prasad, and I. Kao, J. Tribol. **122**, 394 (2000).
[5] F. Yang and I. Kao, ASME J. Electron. Packag. **123**, 254 (2001).
[6] C. Funke and H. J. Möller, Freiberger Forschungshefte, B **327**, 206 (2004).
[7] H. J. Möller, Adv. Eng. Mater. **6**, 501 (2004).
[8] C. Funke and H. J. Möller, in: Proceedings 19th European PV Solar Energy Conf., WIP – München, ETA – Paris, 2004, p. 1266.
[9] I. Kao, S. Wei, and P. Chiang, in: Proceedings of NSF Design & Manufacturing Grantees Conf., Seattle, WA, 1997, p. 239.
[10] M. Buijs and K. Korpel-van Houten, Wear, **166**, 237 (1993).
[11] M. Buijs and K. Korpel-van Houten, J. Mater. Sci. **28**, 3014 (1993).
[12] A. G. Evans and D. B. Marshall, in: Fundamentals of Friction and Wear (ASM, Metals Park, OH, 1981), p. 441.
[13] S. Malkin and J. E. Ritter, ASME, J. Eng. Ind. **111**, 167 (1989).
[14] B. Lawn, in: Fracture of Brittle Solids (Cambridge University Press, 1993).
[15] M. Verspui and G. de With, J. Europ. Ceram. Soc. **17**, 473 (1997).
[16] B. J. Hamrock, in: Fundamentals of Fluid Film Lubrication, NASA Ref. Publication 1225 (McGraw-Hill, New York, 1991).

